Beam-Deflection Using Gradient Refractive-Index Media for 60 GHz End-Fire Antenna

Abdolmehdi Dadgarpour, Behnam Zarghooni, Bal S.Virdee, and Tayeb A. Denidni

***Abstract*—This paper describes a beam tilting technique for planar dipole antennas utilizing gradient refractive-index metamaterial (GRIM) unit-cells. Beam deflection mechanism is based on the phase shift phenomena resulting from the interaction of the EM waves with media of different refractive-indices implemented using GRIM unit-cells. The GRIM unit-cell comprises of a stub loaded I-shaped resonant structure that is directly integrated onto the dipole antenna. The simulation and experimental results show that an antenna with a 5×4 array of GRIM unit-cells can steer the main beam in the E-plane by +26^{o}with respect to the end-fire direction over 57–64 GHz. The antenna exhibits4dB gain enhancement and S_{11}better than -10 dB from 57–64 GHz. It is also shown that a quad-feed dipole antenna with GRIM arrays can deflect the beam by ±56^o.**

***Index Terms*—Metamaterials, beam steering, dipole antenna, millimeter-wave.**

I. Introduction

THE 60GHz unlicensed frequency band has attracted considerable attention in the light of its large frequency band (57–64 GHz) and high absorption loss. Operation at this frequency band enables reduction of interference as well as greater frequency reuse factor. These characteristics make it very attractive for short-range wireless indoor communication and multi Gb/s data rate systems. One major challenge in the implementation of 60GHz wireless systems is high path-loss, which can be compensated using high gain antennas. However, high gain antennas possess a narrow beamwidth that makes beam alignment difficult, especially where the location of transmitter or receiver is not fixed. Adaptive antennas provide a solution to negate this issue but this is costly [1]-[2]. Another viable technique to re-direct the main beam towards specific direction is based on liquid crystalphased array using reflection-type phase shifter [3] however the scanning is limited to 27^o. This can be overcome using a beam forming network like the Butler matrix [4]-[6] but this can increase the overall system size.

The planar 60 GHz switched beam patch antenna in [4] is implemented using a 4×4 Butler matrix that can switch the direction of the main beam in four directions. This antenna has dimensions 13.1×9.75 mm^2.To realize 2D beam scanning, the authors in [5] used a switched beam network using a pair of 4×4 Butler matrix interconnected to four hybrid couplers, which are connected to a 2×4 patch array to produce eight beam-states. Loading a varactor diode between parasitic elements is another approach to steer the main beam in the azimuth plane with maximum peak gain of 5.9 dB [7]. Another promising method involves integrating a dielectric lens in front of an antenna array for implementing beam steering at millimeter-waves [8, 9].

A. Dadgarpour, B. Zarghooni and T.A. Denidni are with INRS-EMT, Montreal,Quebec,CANADA. (Email: abdolmehdi.dadgarpour@emt.inrs.ca, zarghooni@emt.inrs.ca, denidni@emt.inrs.ca); B.S. Virdee is with Center for Communications Technology at London Metropolitan University, UK.

More recently, the authors in [10] integrated a 4×3 array of high refractive-index metamaterial unit-cells with a bow-tie antenna to demonstrate the feasibility of tilting the direction of the antenna main beam for C-band applications; however the refractive index of the unit-cell could not be altered. With this technique, the antenna exhibits again enhancement of 1.5–2.5 dBi over the frequency range of 7.3–7.7 GHz but the angle of the main beam is limited to 17^o.The authors in [11] presented passive fixed beam forming network (BFN) by applying a 4×4 Butler matrix consisting a SIW phase shifter and coupler to tilt the main beam in both E- and H-planes by 20^o. The antenna consists of a multi-layer structure which is complex to construct and occupies a volume of $2.86\lambda_o \times 2.86\lambda_o \times 0.22\lambda_o$.

This paper presents an inexpensive beam tilting technique using a gradient refractive-index metamaterial (GRIM) unit-cello deflect the direction of the main beam of a 60 GHz end-fire dipole antenna at angles of ±56^o, ±26^o, and 0^o. The unique feature of the GRIM unit-cell is its refractive-index can be altered by varying the stub loading without affecting the overall dimensions of the unit-cell. The proposed antenna consists of a printed dipole antenna incorporating 5×4 array of GRIM unit-cells which are directly integrated onto the antenna along the azimuth plane. Measurements show the deflection of the main beam at angle +26^o and -26^o with respect to the end-fire direction is accompanied by peak gain of 10.2 dB and 9.7 dB, respectively. The antenna radiates with an efficiency of 88% at 60 GHz, which is much higher than the BFN structure in [11] that has an efficiency of 70% at 26.5 GHz. In addition, the proposed antenna exhibits a higher beam tilt angle and a gain enhancement of 4 dB over the frequency range of 57–64 GHz than that in [10] which operates at C-band.

II. Beam Deflection Technique

When an electromagnetic wave (EM) in one medium enters another medium of a different refractive index the wave refracts as predicted by Snell's law. In [12] it is shown that a 2D array of resonators with subwavelength separation results in phase discontinuities in the propagating EM wave as it traverses the interface between two media as predicted by the generalized Snell's law:

$$\sin(\theta_t) n_t = \sin(\theta_i)\, n_i + \frac{\lambda_o}{2\pi}\frac{d\varphi}{dx} \qquad (1)$$

Where θ_i and θ_t are angle of incident and refraction, respectively, and $d\varphi/dx$ is the gradient of phase discontinuity. This principle is employed here to steer the EM radiation emanating from a printed dipole antenna. This is achieved by embedding an artificial media with a higher refractive-index than the antenna, which effectively increases the aperture of the antenna and enhances its gain performance. Authors in [9] have shown it is necessary to offset the antenna from the center of a dielectric lens to create phase differential needed to deflect the waves from the antenna. This approach was implemented here on the printed dipole antenna, as illustrated in Fig. 1. In the initial design a medium of identical refractive-index created using 5×4 array of Type A unit-cells (described in Section III) was integrated in front of an antenna. Both arms of the dipole antenna launch the EM rays, where

each ray has proper effective path length in the aperture of the radiating antenna. The resultant effect of each ray at the far-field can be determined by calculating the array factor (AF) as described in [7] using:

$$AF = 1 + e^{j(kd_1 cos\alpha_1)} + e^{j(kd_2 cos\alpha_2)} \ldots + e^{j(kd_5 cos\alpha_5)} \quad (2)$$

Where $d_1, d_2 \ldots d_5$ are the effective path lengths of each ray emanating from locations $A, B \ldots E$, which can be calculated from the centre of dipole (O) toward the locations $A, B \ldots E$, as shown in Fig.1, where angles $\alpha_1, \ldots \alpha_5$ can be obtained from:

$cos\alpha_1 = \hat{a}_{ro}.\hat{a}_{ra}$=-0.158 $cos\varphi$+0.99 $sin\varphi$
$cos\alpha_2 = \hat{a}_{ro}.\hat{a}_{rb}$=+0.109 $cos\varphi$+0.96 $sin\varphi$
$cos\alpha_3$= 0.363 $cos\varphi$+0.93 $sin\varphi$
$cos\alpha_4$ =0.553 $cos\varphi$+0.83 $sin\varphi$
$cos\alpha_5$ =0.684 $cos\varphi$+0.729 $sin\varphi$

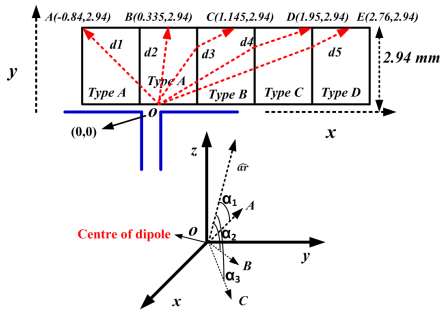

Fig. 1. Ray paths from the offset axis of dipole antenna with 5×4 array of GRIM.

The far-field radiation pattern of the proposed structure in the azimuth plane was calculated as described in [7] by multiplying AF with the element factor of dipole antenna, i.e. $F(\varphi) = \left[\cos\left(\frac{\pi}{2}\cos(\varphi)\right)/\sin(\varphi)\right]$. When the antenna was loaded with identical unit-cells (5×4 array of Type A) the main beam tilted at an angle of 78.5°, as shown in Fig. 2; however when the antenna was loaded with a dielectric slab with 5×4 array of GRIM unit-cells (Types A-D) the main beam deflected to 68°. This is attributed to the phase discontinuity in the GRIM region according to the generalized Snell's law in Eqn. (1), where the effective path length of each ray traversing in GRIM region is different than for identical unit-cell loading.

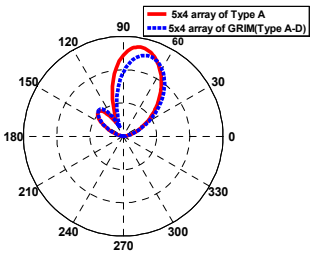

Fig. 2. Radiation patterns of the dipole antenna with dielectric slab constituted from 5×4 array of GRIM unit-cells, and dielectric slab with identical loading.

III. Metamaterial Unit-Cell

The configuration of proposed GRIM unit-cell structure, shown in Fig. 3, is in fact a modified version of the I-shaped resonator in [10] which is loaded with a rectangular stub to provide a specific refractive-index. The dimensions of the stub (L_{load},W_{load}) determine the refractive-index of the medium within its locality over a specific frequency range. This structure was selected because of its ease of integration onto the antenna substrate without altering the antenna profile.

The GRIM unit-cell was constructed on a Rogers RT5870 substrate with the thickness (h) of 0.254 mm, permittivity (ε_r) of 2.3, and loss-tangent of 0.0009.Although the manufacturer recommends the substrate be used for applications up to 40 GHz, the simulated and measured results presented later show it is indeed suitable for applications up to 64 GHz.

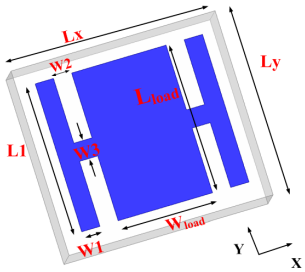

Fig.3.Geometry of the proposed GRIM unit-cell implemented on a dielectric substrate.

The constitutive parameters of GRIM unit-cell, i.e. permittivity, permeability as well as refractive-index, were extracted using Ansoft HFSS, where the PEC and PMC boundary conditions were applied along the *yz* and *xy*-planes, and the two ports were located in *x*-direction. The GRIM unit-cell's effective magnetic permeability and electric permittivity were extracted from the structures transmission and reflection coefficients using the algorithm in [13] which employs Kramers–Kronig relations to estimate the real part of the refractive-index. In order to determine how the refractive-index is influenced by loading the I-shaped unit-cell with a rectangular stub, various unit-cells were developed whose dimensions (in mm) are given in Table I.

Table I Dimensions of GRIM unit-cell of various sizes

Type A	$L1$=0.63, $W2$=0.07, $W1$=0.077, L_x=0.80, L_y=0.72, $W3$=0.08 W_{load}=0.40, L_{load}=0.65, α=(L_{load}/W_{load})=1.62
Type B	W_{load}=0.35, L_{load}=0.56, α=1.62
Type C	W_{load}=0.29, L_{load}=0.47, α=1.62
Type D	W_{load}=0.23, L_{load}=0.37, α=1.62

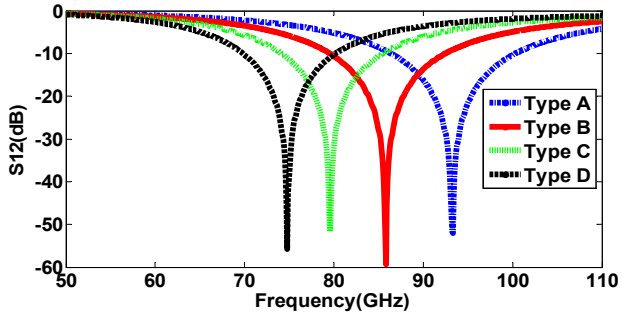

Fig. 4. Magnitude of S_{12} of the proposed GRIM unit-cell structure.

The insertion-loss (S_{12}) response for the various GRIM unit-cells is shown in Fig. 4. Contrary to conventional behavior it is

observed that as the dimensions of the stub loading are reduced the structures anti-resonant frequency shifts downwards in frequency from 93 GHz to 74.5 GHz. This is achieved without affecting the overall dimensions of the GRIM unit-cell. Fig. 4 shows the anti-resonant frequency of Type A unit-cell is far away from the operating band (57–64 GHz), and its effective refractive-index over 57–64 GHz shown in Fig. 5 varies between 1.44 and 1.57, which can be considered virtually constant. However, a larger variation in the effective refractive-index is observed when the unit-cell's anti-resonance is located closer to the operating band, as exemplified by Type D unit-cell. In this case the magnitude of the effective refractive-index varies between 1.73 and 2.4 over 57–64 GHz, as shown in Fig. 6. The above results confirm a graduated refractive-index can be achieved by controlling the length and width of loaded rectangular stub in the I-shaped unit-cell.

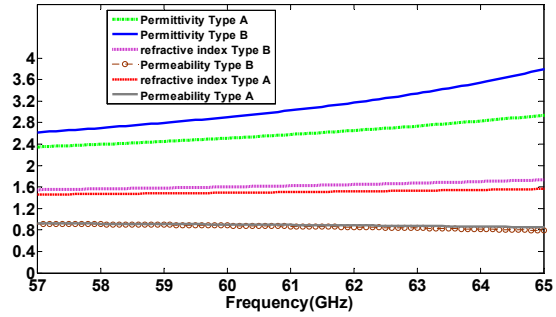

Fig. 5. Relative permittivity, permeability and refractive-index of Type A and B elements.

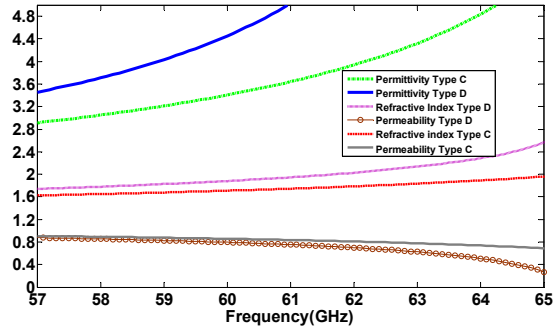

Fig. 6. Relative permittivity, permeability and refractive-index of Type C and D elements.

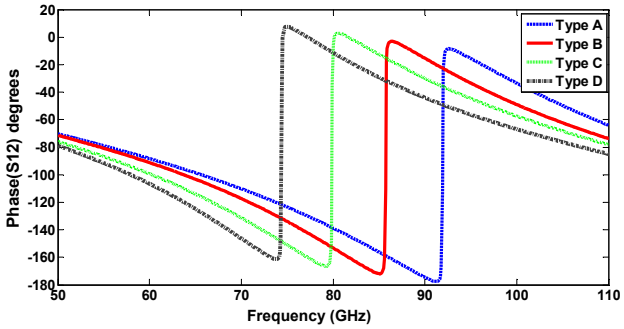

Fig. 7. Phase of the proposed GRIM unit-cell structure.

The GRIM structures exhibit a different phase response across 50–73 GHz, as shown in Fig. 7, where the phase of Type D element lags C, Type C lags B, and Type B lags A. The results show proposed Type of unit-cell has different phase response and therefore will contribute towards a larger tilt angle according to the generalized Snell's law.

IV. Single Dipole Antenna With GRIM Unit-Cell

In this section, the characteristics of a single-dipole antenna are explored when integrated with the proposed gradient refractive-index GRIM unit-cell. The dipole antenna used here is a modified version of the dipole antenna reported in [14]. A 5×4 array of GRIM unit-cells were incorporated into the antenna substrate and laid in front of the dipole-antenna in the azimuth plane, as shown in Fig. 8. The structure of GRIM was separated into the top and bottom layers to enhance coupling with the dipole arms and ensure GRIM effectively interacted with radiation on both sides of the antenna. The dimensions of the proposed antenna are annotated in Fig. 8. The radiation pattern of the printed dipole antenna is shown in Fig. 9 with and without GRIM inclusions in the E-plane of the antenna. The results in Fig. 9 show that when the GRIM is integrated into antenna substrate the direction of the main beam in the E-plane is tilted by 26° with respected to the end-fire direction. In addition, this is accompanied by 4 dB gain enhancement compared to the dipole printed-antenna with no GRIM loading since the radiating aperture size is larger.

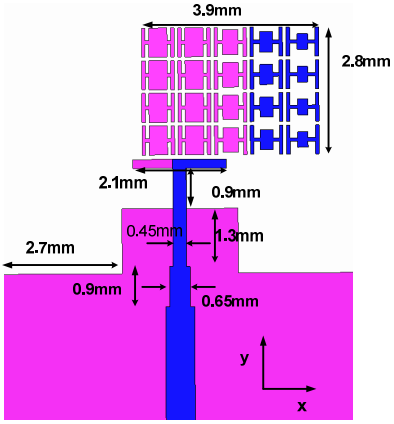

Fig. 8. Configuration of proposed antenna embedded with GRIM unit-cells on the top and bottom surface of substrate.

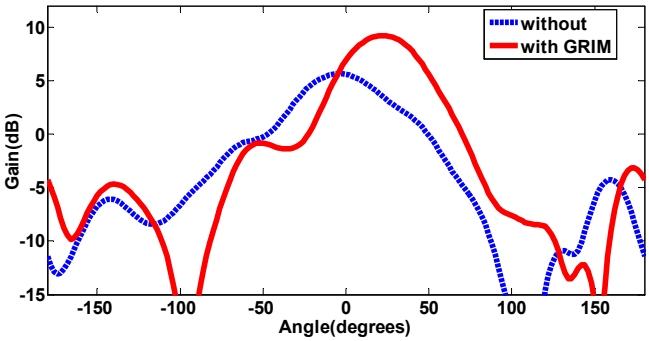

Fig. 9. Radiation patterns of proposed antenna in the E-plane (*xy*) with GRIM unit-cells and a conventional dipole antenna at 60 GHz.

In order to gain a better understanding of the mechanism behind beam tilting, the antenna's Poynting vector was computed with and without GRIM loading using 3D full-wave simulator EM simulation. The results in Fig. 10 show that the

presence of GRIM causes the EM waves to deflect towards the metamaterial region.

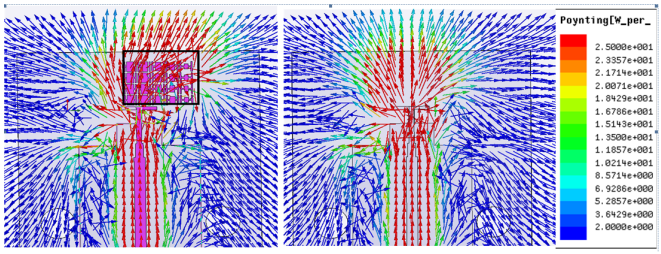

(a) (b)

Fig.10. Poynting vector distribution over the antenna at 60 GHz: (a) with GRIM, and (b) without GRIM.

V. Parametric Study

The effect of GRIM unit-cell columns on the beam tilting is now investigated. Initially the antenna was loaded with two columns of four unit-cells (4×2 arrays of Type A unit-cell) with the same refractive-index (n_1) in front of dipole antenna. The configuration directs the radiation pattern towards the end-fire direction as shown in Fig. 11. By increasing the columns to 3, 4, and 5 with different refractive indices (n_3,n_4,n_5) results in the main beam to tilt by 8°, 16°, and 26°, respectively, as shown in Fig. 11. Six GRIM columns provide a beam tilt of 29°, however this is accompanied by a marginal gain dropped and deterioration in SLL. Hence 5 columns (5×4 GRIM) were selected in the final design.

The effect on the beam angle by offsetting the dipole feed along the *x*-direction was investigated. The feed of the dipole antenna with 5×4 GRIM was offset in the +*x* direction in steps of 0.5 mm from 0 to 3 mm which resulted in the main beam shifting from -25° to 25° as shown in Fig.12.

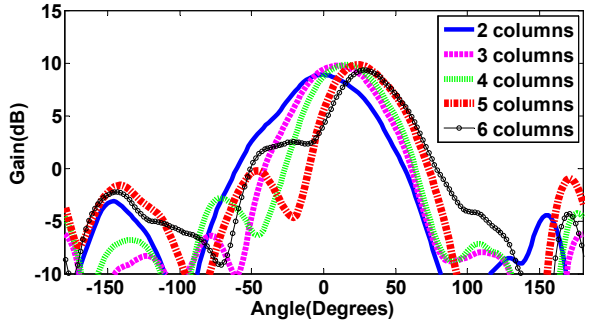

Fig. 11. Radiation pattern of antenna as a function of number of GRIM unit-cell columns.

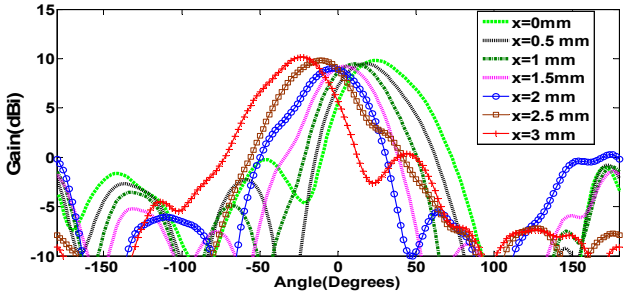

Fig. 12. Radiation pattern for a 5×4 GRIM as a function of feed-line offset along the *x*-direction at 61 GHz.

The E-plane (*xy*) radiation pattern at 61 GHz of the dipole antenna with a dielectric slab loaded with 5×4 array of GRIM unit-cells (Types A-D), and with 5×4 array of identical unit-cells (Type A) is shown in Fig. 13. This figure shows the main beam of the antenna is deflected by 29° when an array of GRIM unit-cells is integrated on dielectric slab. There is a 9° difference between the two scenarios, and the antenna with GRIM loading provides 1.1 dBi more gain than when loaded with an array of identical unit-cells.

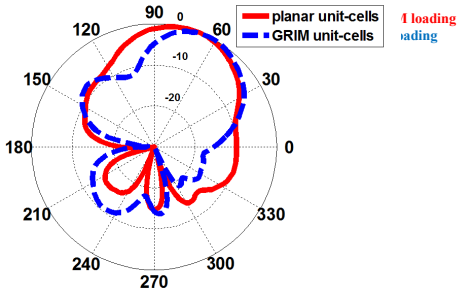

Fig. 13. Radiation pattern of antenna having dielectric slab loaded with GRIM unit-cells and slab with identical unit-cells.

VI. Experimental Results

The proposed single dipole-antenna with a 5×4 array of gradient refractive-index metamaterial unit-cells was fabricated and its performance measured. The photograph of the prototype dipole antenna with GRIM loading is shown in Fig. 14(a).There is good correlation between the simulated and measured reflection-coefficient results, shown in Fig. 14(b), and the discrepancy in the measured response is attributed to the fabrication tolerance. The results confirm that the reflection-coefficient is better than -10 dB between 57–64 GHz. A 1.85 mm end-launch connector (model no.1893-03A-5) was used for the measurement.

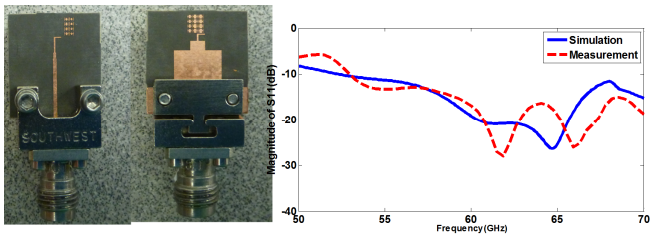

(a) (b)

Fig. 14. (a) Photograph of dipole antenna with GRIM array, and (b) simulated and measured reflection coefficient.

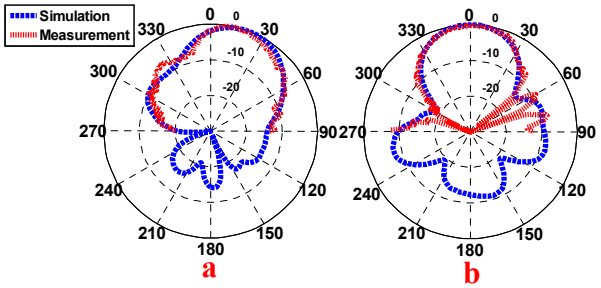

Fig.15.The normalized radiation pattern of single dipole-antenna with a 5×4 array of GRIM loading at 60 GHz in the (a) E-plane (*xy*), and (b) H-plane (*yz*).

The simulated and measured radiation pattern of the single dipole antenna with GRIM loading in the E-plane at 60 GHz is shown in Fig. 15(a). The main beam of the antenna is

confirmed to tilt by 26°. The radiation pattern in the H-plane at 60 GHz remains unchanged, as shown in Fig. 15(b), and is oriented towards the end-fire direction.

VII. Double-Feed Antenna With 5×4 Array Of GRIM

The versatility of proposed approach can be demonstrated by using a beam switching network to steer the main beam from +26° to -26°. To achieve this requirement an additional dipole-antenna was added to the proposed single GRIM loaded dipole-antenna, as shown in Fig. 16. This configuration includes of a double-dipole antenna with a 5×4 array of GRIM unit-cells. The operation of this structure is based on the concept explained in Section II. When antenna-1 is excited with the GRIM loading placed off-center to the right of dipole antenna then the main beam is tilted towards the GRIM region by +26°. When port 1 is terminated with a 50 ohm load and antenna-2 is excited, as the GRIM unit-cells are off-center to left of antenna-2, the main beam tilts towards the GRIM region by -26°. When both ports are excited the main beam propagates towards the end-fire direction (+*y*).

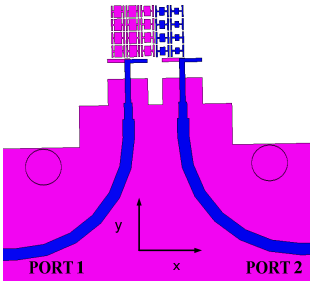

Fig. 16. Geometry of double-feed antenna with 5×4 array of GRIM unit-cells.

The measured reflection-coefficient of the two ports, shown in Fig. 17, is better than -10 dB in the frequency range of 57–64 GHz. The results of simulated radiation pattern of three states (-26°, 0°, +26°) at 61 GHz are shown in Fig. 18.

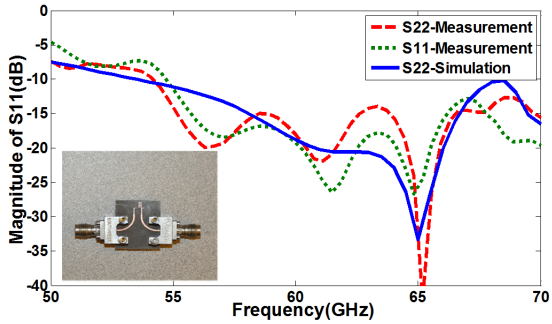

Fig. 17. The measured reflection-coefficient of the double dipole GRIM antenna with inset photograph of fabricated antenna.

The radiation pattern in the azimuth plane was measured by exciting one port at a time using an end-launch connector while the other connector was terminated. The measured and simulated normalized radiation pattern in the azimuth plane (E-plane) at 58, 61, and 63 GHz is shown in Fig. 19(a-c). There is good correlation between the simulation and measured results. Fig. 19(d) shows the normalized radiation pattern in the H-plane at 60 GHz is oriented along the end-fire direction.

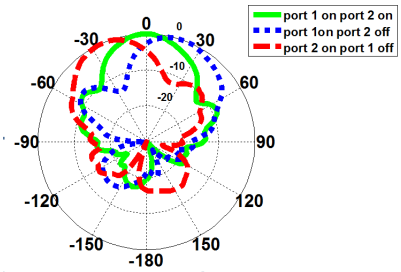

Fig. 18. The simulated normalized radiation pattern when beam is switched in three states +26°, 0°, and -26° at 61 GHz.

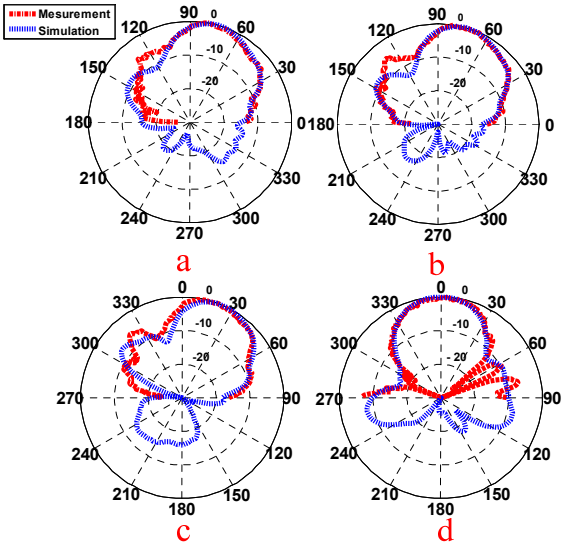

Fig.19. Normalized radiation pattern of proposed antenna with GRIM loading in the E-plane when port 1 is excited at: (a) 58 GHz, (b) 61 GHz, (c) 63 GHz, and (d) with GRIM loading in the H-plane at 60 GHz.

The simulated and measured radiation pattern of the antenna when port 2 is excited and port 1 is terminated is shown in Fig. 20. The result confirms that the main beam direction is tilted by -26° as expected. The antenna gain was measured using the comparative method that involves measuring the signal received by the reference antenna and the test antenna, and determining the relative difference in the gain of both antennas. With this information the gain of the test antenna was determined. The measured radiation efficiency was calculated as explained in [11]. The measured gain of double feed antenna at different beam scan angles along with efficiency are given in Table II. The measured result indicates that there is a maximum peak gain of 10.2 dB at 61 GHz, when the beam is tilted by +26°.

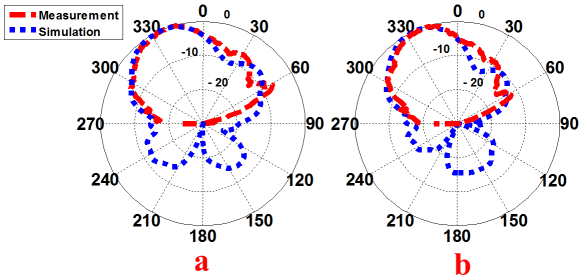

Fig. 20. Normalized radiation pattern of proposed antenna with GRIM loading in E-plane when port 2 is excited at: (a) 59 GHz, and (b) 63 GHz.

Table II - Measured peak gain and efficiency of double feed GRIM antenna

Freq. (GHz)	Simulated peak gain at angle $+26^o$	Measured peak gain at angle $+26^o$	Simulated peak gain at angle -26^o	Measured peak gain at angle -26^o	Measured radiation efficiency (%)
58	9.60	9.4	9.30	9.40	87.5
61	9.90	10.2	9.72	9.70	88.0
63	9.70	10.0	9.75	9.70	84.0

VIII. Four-Feed Antenna With GRIM Array

In Section VII it was shown that a double feed antenna with 5×4 GRIM enables the main beam of antenna to be steered from $-26^o$to $+26^o$. In order to achieve greater scan coverage the configuration in Fig. 21 is proposed.

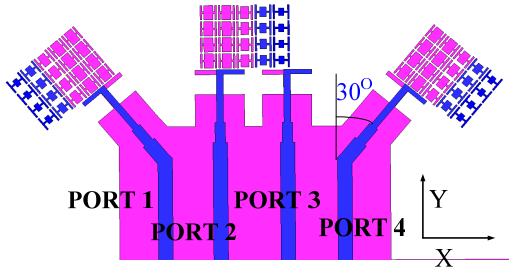

Fig. 21. Configuration of double-feed antenna with 5×4 GRIM unit-cells.

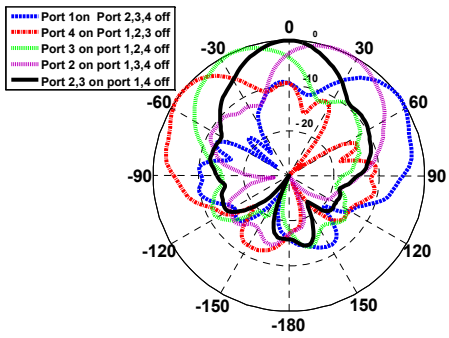

Fig. 22. Radiation pattern of proposed four-feed antenna with GRIM array in E-plane to realize five angle beam switching at 61 GHz.

The structure consists of four feed-lines where the outer two feed-lines are tilted by 30^o with respect to the *y*-axis. The associated 5×4 array of GRIM unit-cells is also tilted by 30^o. The operation of quad-feed structure is similar to the double-feed configuration. Fig. 22 shows the total radiation pattern of antenna configuration in different states, proving that beam switching is achievable at $\pm 56^o$, $\pm 26^o$, and 0^o.

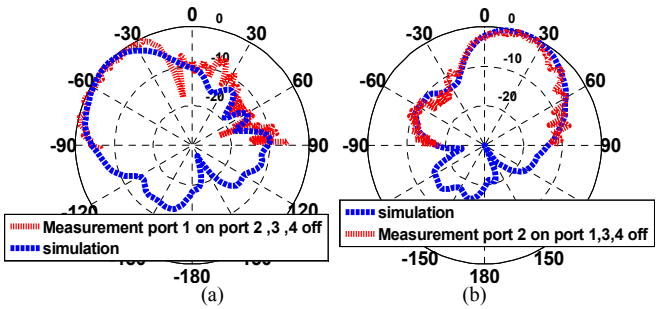

Fig. 23. Radiation pattern at 60 GHz of the quad-feed antenna when (a) port 1 is excited, and (b) port 2 is excited.

In order to validate the simulation results the radiation pattern of two states was measured at 60 GHz as shown in Fig. 23. In the first state, port 1 is excited and the other ports are terminated, resulting in the main beam deflecting by -56^o. A piece of absorbing material was attached to the other ports to prevent the radiation from other ports. In the second state, port 2 was excited and the other ports were terminated. In this case the main beam tilted by $+26^o$.

IX. Conclusion

Gradient refractive-index metamaterial (GRIM) structure was used to deflect the direction of the main beam of a dipole antenna by a specified angle. This was achieved by integrating 5×4 array of GRIM unit-cells on the planar antenna. The GRIM unit-cell comprise of an I-shaped structure loaded with a rectangular stub, where the dimensions of the stub loading determine the refractive index of the unit-cell. The measured results confirm the direction of the main beam to deflect by $+26^o$ in the E-plane with gain enhancement of 4 dB resulting from the increased size of the radiating aperture. A double-feed dipole with 5×4 GRIM unit-cells was used to demonstrate scanning of the main beam in the E-plane from -26^o to $+26^o$. Using the proposed technique a quad-feed antenna was shown to provide beam tilt angles of $\pm 56^o$, $\pm 26^o$, and 0^o.

References

[1] N. Celik, M.F. Iskander, R. Emrick, S.J. Franson, J. Holmes, "Implementation and experimental verification of a smart antenna system operating at 60 GHz band," IEEE Trans. Antennas Propag., vol.56, no.9, pp.2790-2800, Sep. 2008.

[2] G. Grosskopf, R. Eggemann, H. Ehlers, A. Kortke, et al., "Maximum directivity beam-former at 60 GHz with optical feeder," IEEE Trans. Antennas Propag., vol.51, no.11, pp.3040-3046, Nov. 2003.

[3] P. Deo, D. Mirshekar-Syahkal, L. Seddon, S.E. Day, F.A. Fernández, "60 GHz liquid crystal phased array using reflection-type phase shifter," European conf. on Antennas and Propag., pp. 927-929, April 2013.

[4] C-H. Tseng, C-J. Chen, T-H. Chu, "Alow-cost 60-GHz switched-beam patch antenna array with butler matrix network," IEEE Antennas and Wireless Propagation Letters, vol.7, pp.432-435, 2008.

[5] W.F. Moulder, W. Khalil, J.L. Volakis, "60-GHz two-dimensionally scanning array employing wideband planar," IEEE Antennas and Wireless propagation letters, vol.9, pp.818-821, 2010.

[6] H. Chu, Y-X. Guo, Z. Wang "60-GHz LTCC wideband vertical off-center dipole antenna and arrays," IEEE Trans. Antennas Propagat., vol.61, no.1, pp.153-161, Jan. 2013.

[7] Md. R. Islam, and M. Ali, "A 900 MHz beam steering parasitic antenna array for wearable wireless applications," IEEE Trans. Antennas Propag., vol. 61, no. 9, pp.4520-4527, Sept. 2013.

[8] A. Artemenko, A. Maltsev, A. Mozharovskiy, A. Sevastyanov, V. Ssorin, R. Maslennikov, "Millimeter-wave electronically steerable integrated lens antennas for WLAN/WPAN applications," IEEE Trans. Antennas propagat., vol.61, no.4, pp. 1665-1671, Apr. 2013.

[9] D.F. Filipovic, G.P. Gauthier, S. Raman, and G.M. Rebeiz, "Off-axis properties of silicon and quartz dielectric lens antennas," IEEE Trans. Antennas Propag., vol. 45, no. 5, pp. 760–766, May 1997.

[10] A. Dadgarpour, B. Zarghooni, B.S. Virdee, T.A. Denidni, "Beam tilting antenna using integrated metamaterial loading," IEEE Trans. Antennas Propagat., vol.62, no.5, pp. 2874-2879, May 2014.

[11] A.J. Guntapalli, T. Dejerafi, K. Wu, "Two dimensional scanning antenna array driven by integrated waveguide phase shifter," IEEE Trans. Antennas Propagat., vol.62, no.3, pp. 1117-1123, March 2014.

[12] N. Yu, P. Genevet, M.A. Kats, F. Aieta, J.P. Tetienne, et al., "Light propagation with phase discontinuities: Generalized laws of reflection and refraction," Science, vol. 334, pp. 333-337, Oct. 2011.

[13] Z. Szabó, P.G. Ho, R. Hedge, E.P. Li, "A unique extraction of metamaterial parameters based on Kramers-Kronig relationship," IEEE Trans. Microw. Theory Tech., vol.58, no.10, pp.2646-2653, Oct.2010.

[14] R.A. Alhalabi, G.M. Rebeiz, "High-gain Yagi-Uda antennas for millimeter-wave switched-beam systems," IEEE Trans. Antennas Propagat., vol.57, no.11, pp. 3672-3676, Nov. 2009.